

# Effects of coupling between octahedral tilting and polar modes on the phase diagram of $\text{PbZr}_{1-x}\text{Ti}_x\text{O}_3$

F. Cordero,<sup>1</sup> F. Trequattrini,<sup>2</sup> F. Craciun<sup>1</sup> and C. Galassi<sup>3</sup>

<sup>1</sup> CNR-ISC, Istituto dei Sistemi Complessi, Area della Ricerca di Roma - Tor Vergata,  
Via del Fosso del Cavaliere 100, I-00133 Roma, Italy

<sup>2</sup> Dipartimento di Fisica, Università di Roma "La Sapienza", P.le A. Moro 2, I-00185 Roma, Italy and

<sup>3</sup> CNR-ISTEC, Istituto di Scienza e Tecnologia dei Materiali Ceramici, Via Granarolo 64, I-48018 Faenza, Italy

(Dated:)

The results are presented of anelastic and dielectric spectroscopy measurements on  $\text{PbZr}_{1-x}\text{Ti}_x\text{O}_3$  (PZT) with compositions near the two morphotropic phase boundaries (MPBs) that the ferroelectric (FE) rhombohedral phase has with the Zr-rich antiferroelectric and Ti-rich FE tetragonal phases. These results are discussed together with similar data from previous series of samples, and reveal new features of the phase diagram of PZT, mainly connected with octahedral tilting and its coupling with the polar modes.

Additional evidence is provided of a new phase transformation, whose temperature  $T_{\text{IT}}(x)$  prosecutes the long range tilt instability line  $T_{\text{T}}(x)$  up to  $T_{\text{C}}$ . It is interpreted as an initial stage of the tilt instability, and it is proposed that the difficulty of seeing the expected  $\frac{1}{2}\langle 111 \rangle$  modulations in diffraction experiments is due to the anisotropy in the correlation length for octahedral tilting around  $\langle 100 \rangle$ , which, in the presence of enhanced lattice disorder near the AFE border favours precursor clusters of octahedra that exhibit mainly  $\frac{1}{2}\langle 100 \rangle$  modulation. It is shown that the lines of the tilt instabilities tend to be attracted and merge with those of polar instabilities. Not only  $T_{\text{IT}}$  bends toward  $T_{\text{C}}$  and then merges with it, but in our series of samples the temperature  $T_{\text{MPB}}$  of the dielectric and anelastic maxima at the rhombohedral/tetragonal MPB does not cross  $T_{\text{T}}$ , but deviates remaining parallel or possibly merging with  $T_{\text{T}}$ . These features, together with a similar one in  $(\text{Na}_{1/2}\text{Bi}_{1/2})_{1-x}\text{Ba}_x\text{TiO}_3$ , are discussed in terms of cooperative rather than competitive coupling between tilt and FE instabilities, which may trigger a common phase transition. An analogy is found with recent simulations of the tilt and FE transitions in multiferroic  $\text{BiFeO}_3$  [Kornev and Bellaiche, Phys. Rev. B **79**, 100105 (2009)].

An abrupt change is found in the shape of the anelastic anomaly at  $T_{\text{T}}$  when  $x$  passes from 0.465 to 0.48, whose possible implications on the existence of a rhombohedral/monoclinic boundary are discussed.

## I. INTRODUCTION

The phase diagram of the most widely used ferroelectric perovskite  $\text{PbZr}_{1-x}\text{Ti}_x\text{O}_3$  (PZT) still has unclear features (for the phase diagram, see Fig. 6). It has been known since the fifties<sup>1-3</sup> and the major recent discovery was the existence of a monoclinic (M) phase<sup>4</sup> in a narrow region at the morphotropic phase boundary (MPB) that separates the ferroelectric (FE) Zr-rich rhombohedral (R) region from the Ti-rich tetragonal (T) one. In the M phase the polarization may in principle continuously rotate between the directions in the T and R domains, so providing an additional justification for the well known and exploited maximum of the electromechanical coupling at the MPB. The existence of domains of M phase is actually still debated, the alternative being nanotwinned R and/or T domains that over a mesoscopic scale appear as M.<sup>5,6</sup> Since experimental evidences for both types of structures exist, the possibility should be considered that genuine M domains and nanotwinning coexist at the MPB, being both manifestations of a free energy that becomes almost isotropic with respect to the polarization.<sup>7</sup> The part of the MPB line below room temperature has been investigated only after the discovery of the M phase, and is reported to go almost straight to 0 K at  $x \simeq 0.52$ .<sup>8,9</sup>

Recent studies are also revealing new features of how the  $\text{TiO}_6$  and  $\text{ZrO}_6$  octahedra tilt at low temperature. The instability of the octahedral network toward tilting is a common phenomenon in perovskites  $\text{ABO}_3$ , usually well accounted for by the mismatch between the B-O and A-O networks.<sup>10-13</sup> In the majority of cases the A-O bonds are softer than the B-O bonds, because they are longer and the cation A shares its valence with 12 nearest neighbors O atoms while B with only 6 of them.<sup>14</sup> Therefore, when the A-O bonds become so short with respect to the stiffer B-O bonds, that the latter do not fit into a cubic lattice, the octahedra, rather than compress become tilted. This occurs almost invariably at lower temperature, since the weaker A-O bonds have larger thermal expansion,<sup>15</sup> and with smaller A or larger B mean cation sizes. In the case of PZT, Zr has a radius 19% smaller than Ti and one expects the tilt instability to occur below a  $T_{\text{T}}(x)$  line that encloses the low- $T$  and low- $x$  corner of the  $x - T$  phase diagram. Indeed, the Zr-rich antiferroelectric compositions are tilted ( $a^-a^-c^0$  in Glazer's notation,<sup>16</sup> meaning rotations of the same angle about two pseudocubic axes in anti-phase along each of them and no rotation around the third axis), below a  $T_{\text{AF}}(x)$  line that goes steeply toward 0 K at  $x \sim 0.05$ . Also at higher Ti compositions tilting is observed ( $a^-a^-a^-$  compatible with the rhombohedral  $R3c$  structure) below a

$T_T$  line that presents a maximum at  $x \sim 0.16$  and whose prosecution to low temperature was not followed beyond  $x = 0.4$  until recently. The prediction from first principles calculations that octahedral tilting occurs also in the M and T phase<sup>17</sup> has been confirmed by anelastic and dielectric,<sup>18</sup> structural,<sup>19</sup> Raman<sup>20</sup> and infra-red<sup>21</sup> experiments. The presence of a low-temperature monoclinic  $Cc$  phase<sup>22</sup> with tilt pattern  $a^-a^-c^-$  intermediate between tilted R and T has been excluded by a recent neutron diffraction experiment on single crystals,<sup>23</sup> where below  $T_T$  coexistence was found of tilted  $R3c$  and untilted  $Cm$  phases. Yet, evidence for the  $Cc$  phase has been subsequently reported on PZT where 6% Pb was substituted with smaller Sr, in order to enhance tilting.<sup>24</sup>

Here we report the results of anelastic and dielectric experiments at additional compositions with respect to our previous investigations, which reveal new features of the phase diagram of PZT, mainly related to octahedral tilting and its coupling with the polar degrees of freedom.

## II. EXPERIMENTAL

Ceramic samples of  $\text{PbZr}_{1-x}\text{Ti}_x\text{O}_3$ , with nominal compositions  $x = 0.062, 0.08, 0.12, 0.40, 0.487, 0.494$  have been prepared with the mixed-oxide method in the same manner as previous series of samples.<sup>7,18</sup> The starting oxide powders were calcined at 800 °C for 4 hours, pressed into bars and sintered at 1250 °C for 2 h, packed with  $\text{PbZrO}_3 + 5\text{wt}\%$  excess  $\text{ZrO}_2$  to prevent PbO loss during sintering. The powder X-ray diffraction did not reveal any trace of impurity phases and the densities were about 95% of the theoretical ones. The sintered blocks were cut into thin bars 4 cm long and 0.6 mm thick for the anelastic and dielectric experiments and discs with a diameter of 13 mm and a thickness of 0.7 mm only for the dielectric measurements were also sintered. The faces were made conducting with Ag paste.

The dielectric susceptibility  $\chi(\omega, T) = \chi' - i\chi''$  was measured with a HP 4194 A impedance bridge with a four wire probe and an excitation of 0.5 V/mm, between 0.1 and 100 kHz. The heating and cooling runs were made at 0.5 – 1.5 K/min between 100 and 800 K in a modified Linkam HFS600E-PB4 stage and up to 540 K in a Delta climatic chamber.

The dynamic Young's modulus  $E(\omega, T) = E' + iE''$  was measured between 100 and 770 K in vacuum by electrostatically exciting the flexural modes of the bars suspended on thin thermocouple wires.<sup>25</sup> The reciprocal of the Young's modulus, the compliance  $s = s' - is'' = 1/E$ , is the mechanical analogue of the dielectric susceptibility. During a same run the first three odd flexural vibrations could be excited, whose frequencies are in the ratios 1 : 5.4 : 13.2. The angular frequency of the fundamental resonance is<sup>26</sup>  $\omega \propto \sqrt{E'}$ , and the temperature variation of the real part of the compliance is given by  $s(T)/s_0 \simeq \omega_0^2/\omega^2(T)$ , where  $\omega_0$  is chosen so that  $s_0$  represents the compliance in the paraelectric phase. The

imaginary parts of the susceptibilities contribute to the losses, which are presented as  $Q^{-1} = s''/s'$  for the mechanical case and  $\tan \delta = \chi''/\chi'$  for the dielectric one.

## III. RESULTS

For clarity, we will consider separately the anelastic and dielectric spectra with compositions in the range  $0.062 < x < 0.2$ , and those in the MPB region. We will present the new data together with those already published in Refs. 7,18.

### A. Octahedral tilting below $T_T$ and $T_{IT}$ : $0.062 < x < 0.2$

Figure 1 presents the dielectric and anelastic spectra measured during heating of  $\text{PbZr}_{0.92}\text{Ti}_{0.08}\text{O}_3$ , a composition where also the new transition at  $T_{IT}$  is clearly visible in the elastic compliance  $s'$ . The comparison between the two types of susceptibilities puts in evidence their complementarity in studying combinations of polar and non polar modes. The dielectric susceptibility  $\chi'$  is of course dominated by the FE transition at  $T_C$  (note the logarithmic scale), it has a very attenuated step below the well known tilt transition at  $T_T$ , and practically nothing visible at  $T_{IT}$ , due to both the broader shape of the anomaly and the proximity to the Curie-Weiss peak. The dielectric losses provide an indirect but more clear mark of the non polar transition at  $T_T$ , presumably through a change in the mobility and/or amplitude of charge and polar relaxations which are affected by octahedral tilting.

The elastic compliance  $s'$ , on the other hand, is only indirectly affected by the FE transition, since strain is not an order parameter of the transition and is linearly coupled to the square of the polarization. The Landau theory of phase transitions<sup>27,28</sup> predicts a step in  $s'$  for this type of coupling, which is indeed observed at higher Ti compositions,<sup>18</sup> but has a strong peaked component in Zr-rich PZT. We do not have an obvious explanation for this peaked response, which is frequency independent and intrinsic, but mechanisms involving dynamical fluctuations are possible.<sup>28</sup> The advantage of a reduced anelastic response to the FE instabilities is that the other transitions are not as masked as in the dielectric case, so that not only is the tilt transition at  $T_T$  clearly visible as a step in  $s'$  and peak in  $Q^{-1}$ , but also the new transition can be detected at  $T_{IT}$  even very close to  $T_C$ . As already discussed,<sup>7</sup> this transition has all the features of the transition at  $T_T$  but in an attenuated and broadened form, so providing further support to an explanation in terms of a disordered precursor to the final long range tilt ordering below  $T_T$ .

The broad peaks and steps in both the dielectric and anelastic losses below  $T_C$  have scarce reproducibility, which indicates their extrinsic origin, namely the motion of domain walls and charged defects, whose state depends

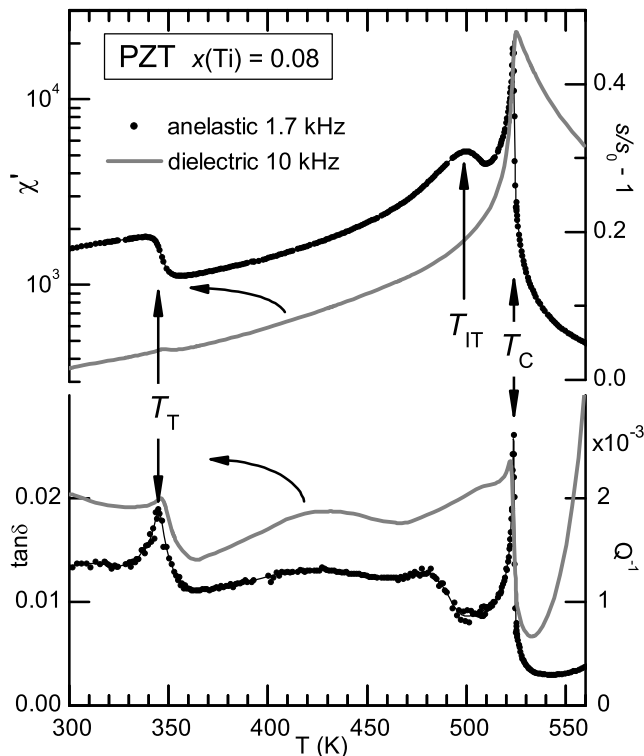


FIG. 1: Dielectric (left ordinates) and anelastic (right ordinates) spectra (higher panel real susceptibilities, lower panel losses) of  $\text{PbZr}_{0.92}\text{Ti}_{0.08}\text{O}_3$  measured during heating.

on the thermal history. Instead, all the features indicated by arrows are completely independent of the measuring frequency, temperature rate and thermal history, and therefore are recognizable as intrinsic effects due to the FE and tilt transitions. Hysteresis between heating and cooling is observed due to the first order character of the transitions and to the presence of domain walls relaxations. Examples of the differences between the features that are intrinsic and stable and those that present dispersion in frequency or are less reproducible have been reported previously<sup>7,18</sup> and are omitted here.

Figure 2 presents the anelastic spectra of PZT with  $0.062 < x < 0.17$ , including compositions already present in Ref. 7. All the curves are similar to the  $x = 0.08$  case of Fig. 1, with the three type of transitions at  $T_C$ ,  $T_{IT}$  and  $T_T$  clearly visible in separate temperature ranges. Both the  $s'$  and  $Q^{-1}$  curves have sharp peaks at the FE transitions, so that the  $T_C$ 's are simply labeled with the compositions in %Ti. The other transition temperatures are indicated by vertical bars centered on the curves and arrows labeled with the respective compositions. The features of  $Q^{-1}$  in the  $T_{IT}$  temperature range are not labeled because are due to the extrinsic contributions mentioned above.

The temperatures of the tilt transition are identified with the upper edges of the steps in the real parts, which generally coincide with a spike or sharp kink in the losses. The rounded step and lack of reproducible anomaly in

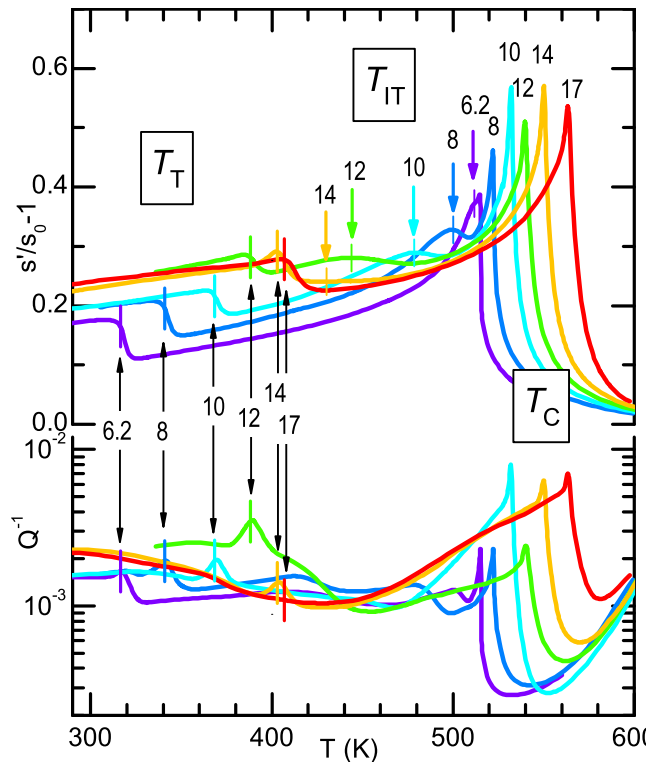


FIG. 2: Elastic compliance  $s'$  and energy loss coefficient  $Q^{-1}$  measured at  $\sim 1.7$  kHz on PZT at the compositions 6.2, 8, 10, 12, 14, 17% Ti, as indicated by the numbers at the phase transitions.

the losses increase the error on  $T_{IT}$ , which however remains small enough to not change the features of the phase diagram discussed later. Due to the importance of the behavior of  $T_{IT}(x)$  in the Discussion, a detail of this anomaly in the  $s'(T)$  curves, including 5% Ti, is shown in Fig 3. An anomaly corresponding to  $T_{IT}$  might be present slightly above  $T_T$  for  $x = 0.17$ , but lacking a clear sign of it, it is assumed to coincide with  $T_T$ . At low  $x$ , the curve of  $x = 0.05$  does not present any clear shoulder below  $T_C$ , and it is assumed  $T_{IT} \equiv T_C$ .

The transition temperatures measured on both heating and cooling are reported in the phase diagram of Fig. 6, where the  $T_{IT}$  line departs from  $T_T$  at  $x \simeq 0.17$ , has a kink centered at  $x = 0.11$  and finally joins the  $T_C$  line at  $0.05 < x < 0.062$ . The new feature that will be the main focus of the present work is the kink and the merging with  $T_C$  at  $x > 0.05$ . It is also noticeable that the anomaly at  $T_{IT}$  becomes more intense and sharper on approaching  $T_C$ .

## B. Compositions near the MPB

As discussed in the previous investigations,<sup>7,18</sup> the MPB in PZT is signaled by a maximum in the dielectric and above all elastic susceptibilities. Again, it is stressed that such maxima are almost independent of fre-

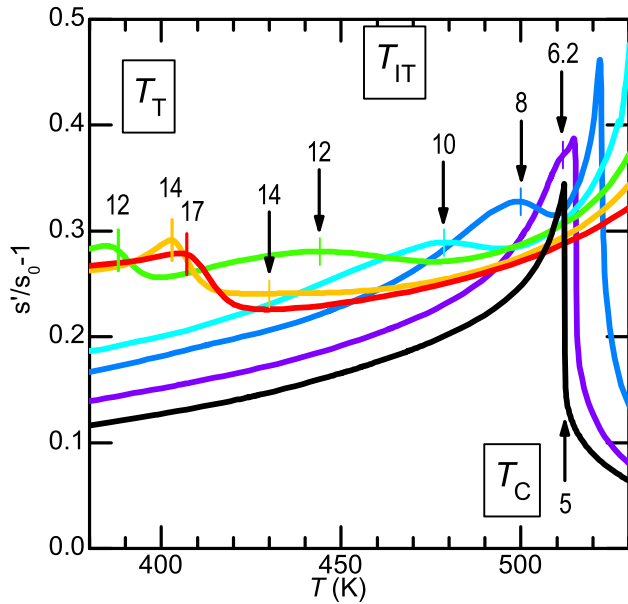


FIG. 3: Detail of the anomalies of the elastic compliance at  $T_{IT}$ , measured at  $\sim 1.7$  kHz during cooling on samples with  $0.05 \leq x \leq 0.17$ . The numbers indicate the compositions in %Ti.

quency and temperature rate, and therefore are intrinsic effects due to the evolution of the order parameter at the MPB and its coupling with strain. Also the losses are rather high in the region of the MPB, but no feature is found that is directly ascribable to the phase transition; rather, their dependence on frequency and thermal history show that they are due to the abundant twin walls and other domain boundaries, whose density and mobility depend on many factors and is maximal around the MPB. Instead, the losses contain clear cusps or steps at the tilt transitions,<sup>7,18</sup> so allowing  $T_T$  to be determined also in the proximity with the MPB, where the real part is dominated by the peak at  $T_{MPB}$ . We therefore discuss separately the real parts of  $\chi$  and  $s$ , containing information on the polar transition at the MPB, and the losses, containing information on the tilt transitions.

### C. Maxima of the susceptibilities at the MPB

Figure 4 is an overview of  $\chi'$  and  $s'$  curves measured during cooling at all the compositions  $x \geq 0.40$  we tested so far.

We call  $T_{MPB}$  the temperatures of the maxima in  $\chi'$  and  $s'$ , marked with vertical bars on the curves. These temperatures do not coincide exactly with each other, because  $\chi'$  and  $s'$  are two different response functions of polarization and strain respectively, but, once plotted in the phase diagram, they present an excellent correlation with the MPB determined by diffraction, at least in the middle of the MPB line (see Fig. 6). The dielectric maxima at  $T_{MPB}$  are much smaller and broader than

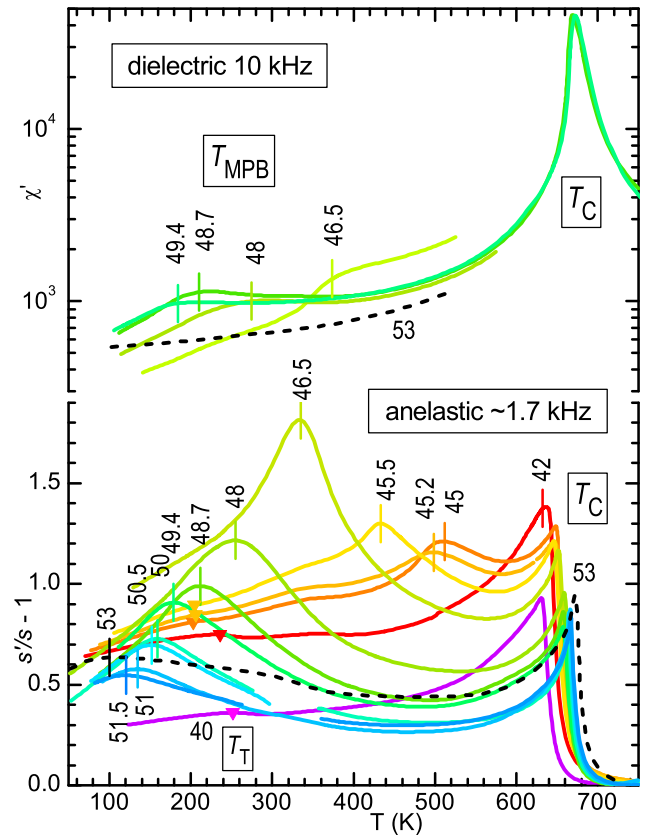


FIG. 4: Dielectric susceptibility and elastic compliance measured during cooling on PZT at the compositions indicated besides the curves in % Ti. The  $T_{MPB}$ 's are indicated with vertical bars and  $T_T$  by triangles (only for  $40 \leq x \leq 45.2$ ).

the Curie-Weiss peak at  $T_C$  (note the logarithmic scale), whereas the anelastic maxima at  $T_{MPB}$  have comparable or even larger intensities than the step at  $T_C$  (part of the peaked component at  $T_C$  has a frequency dispersion denoting relaxation of walls<sup>7,18</sup>).

At  $x = 0.40$  there is no peak attributable to the MPB, but only a minor step below  $T_T$ , which is indicated with triangles up to  $x = 0.452$ ; beyond that composition, the step at  $T_T$  either disappears or is masked by the MPB peak. The other shallow anomaly centred at  $\sim 360$  K in the curves up to  $x \leq 0.465$  is the counterpart of the domain wall relaxation appearing in the losses mentioned above and will be ignored. For  $x \geq 0.45$  the peak at the MPB shifts to lower temperature and develops its maximum amplitude at 0.465, which has been argued to correspond to the point of the phase diagram where the anisotropy of the free energy is minimum.<sup>7</sup> The presence of a peak in  $s'$  at the MPB has also been argued to be evidence that the phase transition occurring at the MPB consists mainly in the rotation of the polarization, from the [001] direction of the T phase toward the [111] direction of the R phase. In fact, in that case the transverse component of  $\mathbf{P}$  acts as order parameter and is almost linearly coupled to a shear strain, inducing a peaked re-

sponse also in the elastic susceptibility.<sup>7,18</sup> This would be an evidence that a monoclinic phase, and not only nanotwinned R and T phases, exists below the MPB. Yet, the smooth shape of the maximum is compatible with an inhomogeneous M phase coexisting and possibly promoted by nanotwinning.<sup>7</sup> In fact, indications continue to accumulate of intrinsic phase heterogeneity near the MPB compositions also on single crystals.<sup>29</sup>

Beyond  $x > 0.465$ , the peak at  $T_{\text{MPB}}$  gradually decreases its amplitude and temperature, and, thanks to the great number of closely spaced compositions, is clearly recognizable as the signature of the MPB up to  $x = 0.515$ . The next composition,  $x = 0.53$  (dashed curves), still has a shallow maximum at a temperature that prosecutes the  $T_{\text{MPB}}(x)$  line, but its nature appears different. In fact, the dielectric  $\chi'$  at the same composition lacks any sign of a maximum, and the overall  $s'$  curve does not any more prosecute the trend of the preceding curves. For this reason, the temperature of this maximum at  $x = 0.53$  is reported in the phase diagram as  $T_{\text{MPB}}$  but accompanied by a question mark. A  $T_{\text{MPB}}$  is extracted also from the curve at  $x = 0.42$ , even though a separate maximum is not present. It is however the only composition where  $s'$  has no sharp feature at  $T_C$ , and we assume that this is due to a rounded peak at  $T_{\text{MPB}}$  very close to  $T_C$ .

#### D. Tilt transition near the MPB

The best signatures of the tilt transition below  $T_T$  are found in the anelastic losses. Figure 5 shows the  $Q^{-1}(T)$  curves at all the compositions  $x \geq 0.40$  we tested so far (only 45.2%Ti is omitted in order to not overcrowd the figure).

The  $T_T$ 's up to  $x = 0.455$  are the same as deduced from the step in the real part, and indicated by triangles in Fig. 4. Up to  $x = 0.465$   $T_T$  is identified with the temperature of a spike in  $Q^{-1}(T)$ , which gradually becomes a cusp and starting from  $x = 0.48$  becomes a large step. As in the previous figures, the  $T_T$ 's are marked by vertical bars centered on the curves and joined by a dashed line, in order to better follow the evolution of the anomaly. The transition between the spike/cusp and the step anomaly is unexpectedly sudden, since it occurs within  $0.465 < x < 0.48$ . Such a discontinuity appears also in the dashed line joining the anomalies, and is marked by an arrow. We emphasize again that the losses generally have a limited reproducibility, because depend on the status of domain walls and defects; therefore, the regularity of the dashed curve joining the tilt anomalies of so many different samples is remarkable and testifies the good and uniform quality of the samples.

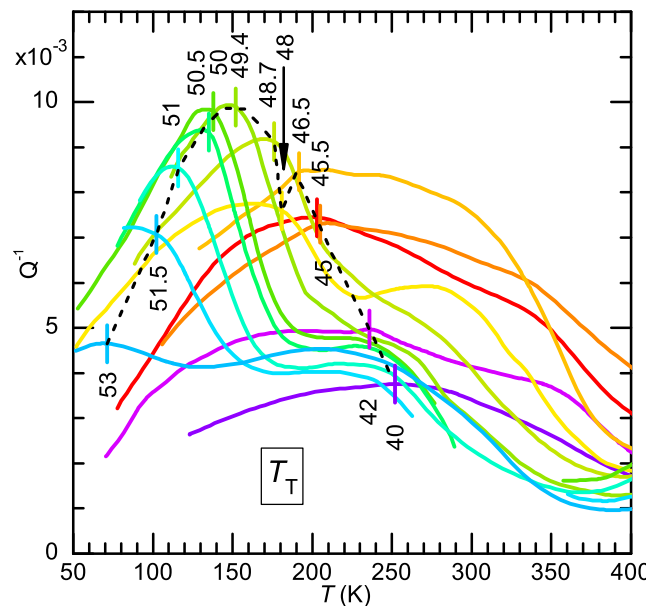


FIG. 5: Elastic energy loss coefficient of PZT at the compositions indicated by the numbers (in %Ti), measured during cooling at  $\sim 1.7$  kHz. The anomalies at  $T_T$  are indicated by vertical bars and joined with a dashed line.

#### IV. DISCUSSION

We refer to the phase diagram of PZT in Fig. 6. Below  $T_C$  and with decreasing Ti content, one finds the following phases:<sup>13,30,31</sup> ferroelectric (FE) tetragonal (T)  $P4mm$  with polarization  $\mathbf{P}$  along  $[001]$ , monoclinic (M)  $Cm$  with  $\mathbf{P}$  rotated toward  $\langle 111 \rangle$ , rhombohedral (R)  $R3m$  with  $\mathbf{P} \parallel \langle 111 \rangle$  and antiferroelectric (AFE) orthorhombic (O)  $Pbam$  with staggered cations shifts along  $\langle 110 \rangle$  and  $a^-a^-c^0$  tilt pattern. Below  $T_T$  octahedral tilt-tilt occurs in all phases.

In Fig. 6, the solid lines join the transition temperatures deduced from our anelastic spectra measured during heating (filled triangles pointing upward), which are generally very close to the points deduced from the dielectric curves (empty triangles). The temperatures measured during cooling are also shown as triangles pointing downward. The figure contains all the data presented here and in Refs. 7,18 and, for completeness, also points obtained at compositions  $x \leq 0.05$ , that will be discussed in a future paper.

The dashed lines are from the most widely published version of Jaffe, Cook and Jaffe<sup>3</sup> with modifications of Noheda *et al.*<sup>8</sup> around the MPB. In a different version<sup>32</sup> the  $T_{\text{MPB}}$  line below  $x = 0.45$  does not prosecute straight up to join  $T_C$  almost perpendicularly, but rapidly decreases its slope and joins  $T_C$  at  $x \sim 0.3$ . At present we have indication of a much smaller deviation of  $T_{\text{MPB}}$  from the datum at  $x = 0.42$  (Fig. 4), but already at  $x = 0.4$  there is no trace of a double transition.

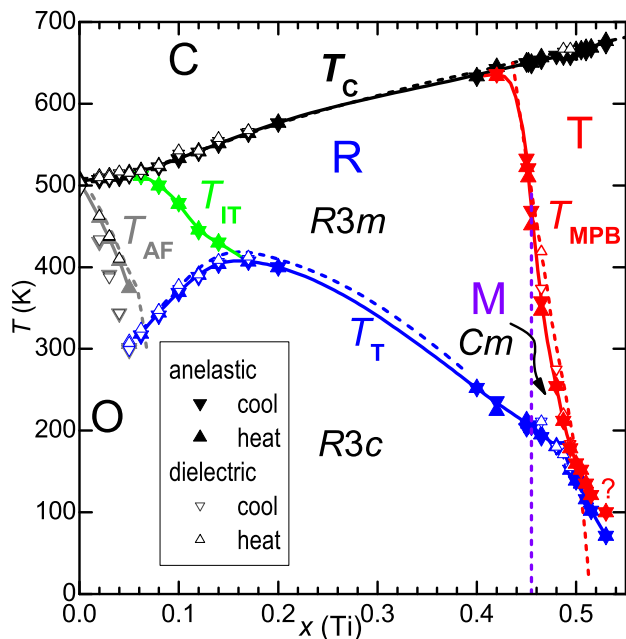


FIG. 6: Phase diagram of PZT based on our anelastic and dielectric spectra. The solid lines join the anelastic data measured during heating; the dashed lines are those from Jaffe and Noheda. The question mark reminds that the shallow maximum of  $s'$  with  $x = 0.53$  at that temperature probably does not signal the MPB crossing.

### A. The octahedral tilt instability

The tendency of the  $\text{BO}_6$  octahedra in  $\text{A}^{2+}\text{B}^{4+}\text{O}_3$  perovskites to tilt has been widely studied and can be rationalized in terms of mismatch between a softer sublattice of longer A-O bonds that compresses a stiffer sublattice of shorter B-O bonds, until the incompressible octahedra tilt in order to accommodate a reduction of the cell and cuboctahedral volume  $V_A$  without reducing their volume  $V_B$ . This effect is quantitatively expressed in terms of the Goldschmidt tolerance factor

$$t = \frac{\overline{\text{A-O}}}{\sqrt{2}\overline{\text{B-O}}} \simeq \frac{r_A + r_O}{\sqrt{2}(r_B + r_O)}$$

which is 1 for the cubic untilted case. In order to predict a tendency to form a tilted phase,  $t$  is written in terms of the ideal ionic radii  $r_X$  of the appropriate valence and coordination, which are tabulated.<sup>33</sup> If  $t < 1$  then the equilibrium B-O bond lengths are too long to fit in a cubic frame of A-O bonds, and tilting occurs below some threshold value; for example, many Sr/Ba based perovskites are tilted when  $t < 0.985$  at room temperature.<sup>12</sup> Alternatively, the polyhedral volume ratio  $V_A/V_B$  is defined,<sup>34</sup> which is 5 for the untilted case and becomes  $< 5$  upon tilting. Of all the normal modes of a cubic perovskite, those that induce a decrease of  $V_A/V_B$  are the combinations of rigid rotations of the octahedra about the cubic axes, while all other normal

modes involve distortions of the polyhedra with little or no change in their volumes.<sup>35</sup> Rotations with all the octahedra in phase along the axis are labeled  $M_3$ , because the staggered shifts of the O atoms create a modulation with vector  $\frac{1}{2}\langle 110 \rangle$ , the M point of the Brillouin zone, while rotations with successive octahedra in antiphase along the axis are labeled  $R_4$ , because the modulation is  $\frac{1}{2}\langle 111 \rangle$ , the R point of the Brillouin zone.<sup>36</sup> These modes are also called antiferrodistortive (AFD), because of the staggered modulation of the atomic displacements, and do not cause the formation of electric dipoles. Most of the low temperature structures of perovskites can be described in terms of combinations of these rotations together with polar modes (shifts of the cations against the O anions). In particular, the low-temperature  $R3c$  rhombohedral phase of PZT, is obtained from the high temperature  $R3m$  ferroelectric R phase, by applying anti-phase rotations of the same angle about all three pseudocubic axes ( $a^-a^-a^-$  in Glazer's notation<sup>16</sup>), while the O-AFE structure  $Pbam$  of  $\text{PbZrO}_3$  is a combination of staggered and hence AFE displacements of the  $\text{Pb}^{2+}$  and  $\text{Zr}^{4+}$  ions along  $[110]$ , with anti-phase tilts along  $[100]$  and  $[010]$  ( $a^-a^-c^0$ ).

In spite of the considerable amount of research on the phase diagram of PZT, little use has been done of these concepts in order to interpret it. Initially the position of the MPB line and its shift to lower  $x$  upon substitution of Pb with La have been discussed in terms of a critical volume of the  $\text{PbO}_{12}$  cuboctahedron, below which the structure changes from T to R.<sup>34</sup> Other investigations on the relationship between MPB and  $t$  in perovskite solid solutions have appeared,<sup>37-39</sup> though without reference to octahedral tilting. Other instances in which ferroelectric perovskites have been studied in terms of the parameter  $t$  are a study of the magnitude of the dielectric permittivity in several Ba and Sr based perovskites.<sup>12</sup>

An indication that the mechanism governing tilting in PZT is indeed the A-O/B-O mismatch is the observation that the substitution of 6%  $\text{Pb}^{2+}$  with the smaller  $\text{Sr}^{2+}$  induces tilting in an originally untilted T phase of PZT, while when codoping with  $\text{Sr}^{2+}$  and  $\text{Ba}^{2+}$ , the latter larger than  $\text{Pb}^{2+}$ , the opposite effects of the two dopants on the average tolerance factor cancel with each other and no tilting is found.<sup>40</sup> When the tilt boundary  $T_T$  has been discussed in terms of  $t$ , the incongruence of the deep depression near the border with the O-AFE phase has been pointed out,<sup>13</sup> and explained in terms of frustration of AFE displacements of the Pb ions perpendicularly to the average FE direction  $\langle 111 \rangle$ . Such displacements lack the long range order of the AFE-O structure, and their frustration would be transmitted to the octahedral tilting through the Pb-O bonds, so lowering the  $T_T$  border in proximity with the AFE-O phase.<sup>13</sup> Certainly the sharp depression in the border to the long range ordering of tilts, the  $T_{AF} + T_T$  line, appears to be caused by some frustration, since it is a typical feature of the phase diagrams with competing states,<sup>41,42</sup> and both the FE/AFE polar modes and different tilt patterns may

be in competition.

The disordered displacements of Pb away from the average polarization have been proposed to occur over the whole R region of the phase diagram and particularly near the other MPB with the T phase, based on the large anisotropic displacement ellipsoids of Pb in Rietveld refinements according to the R structure<sup>43</sup> or to the coexistence of M and R structures.<sup>23,30</sup> While in these cases the Pb displacements off-axis with respect to the  $\langle 111 \rangle$  direction may be imagined as having a FE correlation leading to a rotation of the polarization away from  $\langle 111 \rangle$ , recently a soft mode corresponding to AFE Pb displacements has been found near the MPB of PZT and in relaxor PMN and PZN-PT, suggesting that the AFE-like instability is a common feature of nanoscale domain structures of rhombohedral or pseudorhombohedral lead-based perovskites.<sup>44</sup> Considering that such displacements occur over the whole R region or particularly at the MPBs with the O and the T phases, if they are so strongly coupled with the tilts, one would expect a depression of  $T_T$  also near the MPB with the T phase, which is not observed. There are some possible explanations for the different behavior of  $T_T$  at the two MPBs. One is that the polar displacements away from  $\langle 111 \rangle$  might become static and with larger amplitude and AFE correlation only near the AFE border, so causing the frustration between FE and AFE patterns, while at the MPB to the T-FE phase the AFE correlations remain at the stage of an anomalous phonon softening. On the other hand, it is possible that the main competition occurs between the two different tilt patterns in the R and O phases, since the approaching of the tilt instability to the FE one indicates that in the  $x \rightarrow 0$  region of the phase diagram polar and tilt modes have comparable energetics. It is not evident, however, how the competition between  $a^-a^-c^0$  and  $a^-a^-a^-$  tilt patterns would cause frustration, since they can transform into each other just by switching on and off the anti-phase tilt about the pseudocubic axis  $[001]$ . We believe, however, that the explanation of the  $T_{AF} + T_T$  depression relies on the existence of the additional transformation at  $T_{IT}$ .

### B. The intermediate tilt instability $T_{IT}(x)$ line

The  $T_{IT}$  line appears as the prosecution of the  $T_T$  one toward the lowest  $x$ , or equivalently lowest  $t$ , and highest temperature, and hence it has been identified as the onset of precursor tilting.<sup>7</sup> Presumably, between  $T_{IT}$  and  $T_T$  tilting would be disordered due to the enhanced disorder in the O-Pb-O network near the AFE border, as suggested above.<sup>13</sup> The drastic depression of  $T_T$  would then be due to the fact that most of the mismatch between the Pb-O and (Zr/Ti)-O sublattices is relieved at  $T_{IT}$ , and the final transition to a tilted phase with long range order requires the buildup of sufficient elastic energy in the disordered sublattice of tilted octahedra, that it is convenient to switch to the long range ordered phase. This is

not alternative to the above discussion on the sharp minimum of  $T_{AF} + T_T$  in terms of competing phases. It is simply assumed that the frustration hinders tilting from reaching long range order but not from occurring on the local scale.

This interpretation has not yet been corroborated by a structural study where the onset of tilting below  $T_{IT}$  is actually observed and the tilt pattern is established. Actually, superlattice spots in electron diffraction have been interpreted in terms of in-phase  $M_3$ -type tilts within the otherwise  $R3m$  phase up to  $x \sim 0.15$ .<sup>45,46</sup> That region roughly corresponding to the region delimited by the  $T_{IT}$  border, though a border was not seen.<sup>45,46</sup> These in-phase tilts could not be confirmed by x-ray or neutron diffraction and considerable debate ensued over the interpretation of the electron diffraction  $\frac{1}{2}\langle 110 \rangle$  spots in terms of AFE  $\langle 110 \rangle$  Pb displacements rather than  $M_3$ -type tilts, due to the much weaker strength of the latter and the greater sensitivity of electron diffraction to the damaged surface.<sup>13,47</sup>

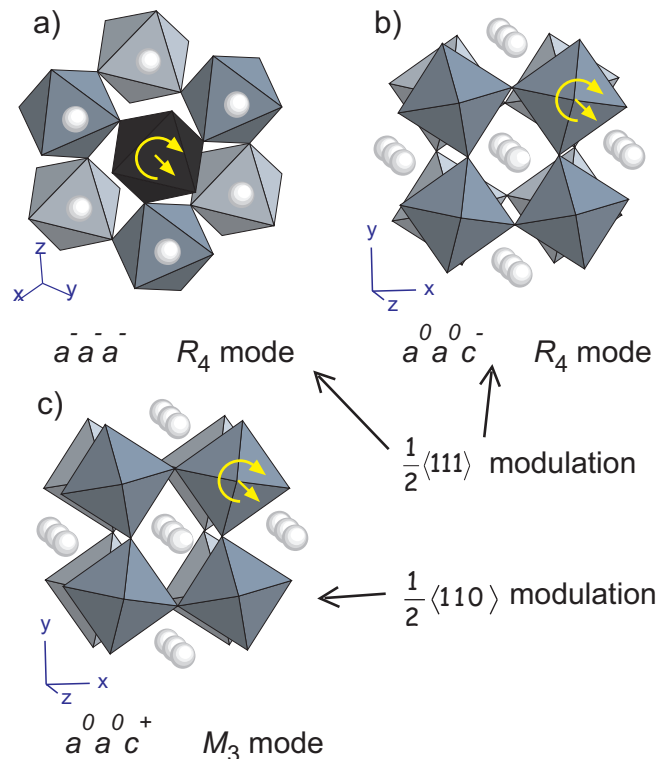


FIG. 7: Three tilt patterns of the  $BO_6$  octahedra. The O ions at the vertices of the octahedra and the B ions at their centers are not shown; the A ions are white. The darker octahedra are in planes closer to the observer. a)  $a^-a^-a^-$  tilt pattern of the  $R3c$  structure seen from a direction close to the  $\langle 111 \rangle$  rotation axis; b) out of phase and c) in phase rotation about the  $[001]$  direction. In b) and c) the octahedra of different planes share only O atoms that do not move under tilting..

The  $M_3$  tilts are in the first place in the search for a mechanism behind the phase transformation at  $T_{IT}$ , because they would cause weak superlattice peaks at po-

sitions coinciding with those from the disordered AFE Pb displacements, so explaining why their onset below  $T_{IT}$  has not yet been noticed. In fact, the disorder in the Pb sublattice, including AFE-like shifts, survives even in the cubic phase, as demonstrated by the observation of electron diffraction  $\frac{1}{2}\langle 110 \rangle$  spots<sup>45,46</sup> and the fact that EXAFS probes the same local environment of Pb<sup>48</sup> and Zr/Ti,<sup>49</sup> both in the FE and in the cubic phases. It seems reasonable to assume that the AFE cation displacements develop their short range order together with the FE order below  $T_C$ , so producing superlattice peaks of the  $\frac{1}{2}\langle 110 \rangle$  type, that mask those from subsequent octahedral tilting below  $T_{IT}$ , if this is of  $M_3$  type. The difficulty with the last assumption is that the final tilting below  $T_T$  is of  $R_4$  type, and the  $M_3$  in-phase tilting is an instability of different type rather than a precursor to it.

1.  $\frac{1}{2}\langle 110 \rangle$  reflections from hindered  $\frac{1}{2}\langle 111 \rangle$  modulation of the tilts?

In order to reconcile the observation of  $M$ -type modulation below  $T_{IT}$  with a more likely short range  $R$ -type modulation, we consider the correlation lengths of the different types of tilting represented in Fig. 7. In a first approximation consider a network of rigid octahedra, that, in order to comply with the mismatch with the Pb-O network, can only tilt without distortions. This is the so-called rigid unit model, whose implications on the anisotropy of the phonon dispersions has been analyzed.<sup>50</sup> Here we focus on the effects that the anisotropy of the correlation length might have on the diffraction patterns.

Consider first the rotation of a single octahedron about one of the cubic axes ( $[001]$  in Fig. 7b) or c)); this will cause a rotation of all the other octahedra in the same plane perpendicular to the axis in an AFD fashion, creating a  $\frac{1}{2}\langle 110 \rangle$  modulation, with a correlation length  $l_B$  which is an increasing function of the B-O bond strength. In the pure rigid unit model  $l_B$  is infinite and there is no correlation at all with the other planes of octahedra, because they share corners of the tilting octahedra only through immobile O atoms. In practice there is an interaction with the adjacent planes through the less energetic B-O-B bond bending and the extensions of the longer and weaker A-O bonds, resulting in a finite correlation length  $l_A$  along the rotation axis, however shorter than  $l_B$ . This means that the correlation volume surrounding an octahedron tilting about a  $\langle 100 \rangle$  direction is a flat disc of diameter  $2l_B$  and thickness  $2l_A$  with  $l_A \ll l_B$ , and this will create superlattice reflections more intense and sharp at  $\frac{1}{2}\langle 110 \rangle$  than at  $\frac{1}{2}\langle 111 \rangle$ . On the other hand, the rotation of an octahedron about a  $\langle 111 \rangle$  axis (Fig. 7a)), as the soft  $R_4$  mode in the  $R3c$  structure, will affect all the surrounding octahedra, which share shifted O atoms both above and below the  $[111]$  plane containing the rotating octahedron. Therefore, for an octahedron rotating about a  $\langle 111 \rangle$  axis the correlation volume is a sphere with diam-

eter  $2l_B$ , containing more octahedra than in the previous case. We therefore postulate that below  $T_{IT}$  the magnitudes of the tilts start becoming so large to cause their propagation through the correlation volume, as for any tilt instability, but this will occur first for those clusters where a deviation toward  $\langle 100 \rangle$  tilt, with smaller correlation volume, is favored by the local cation disorder. In this first stage between  $T_{IT}$  and  $T_T$ , only  $\frac{1}{2}\langle 110 \rangle$  superlattice peaks would appear, easily masked by those from AFE cation correlations. On further cooling below  $T_T$ , the increased instability of the  $R_4$  mode and long range elastic interactions trigger the long range tilt order of the  $R3c$  phase. In other words, in the absence of disorder or frustration  $T_T$  and  $T_{IT}$  would coincide and represent the temperature below which the propagation of the  $a^-a^-a^-$  tilt instability starts. In the presence of disorder, local tilting about  $\langle 100 \rangle$  axes is favored because of its smaller correlation volume; the resulting disordered tilting partially relieves the mismatch between Pb-O and (Zr/Ti)-O bonds, and further cooling below  $T_T$  is necessary in order to reach the long range  $a^-a^-a^-$  ground state. This may explain the deep depression of  $T_T$  below  $x < 0.15$ .

**C. The kink in the tilt instability  $T_{IT}(x)$  line and the effect of coupling of different modes on the phase diagram**

If octahedral tilts and polar modes were independent of each other, the  $T_C$  and  $T_T + T_{IT}$  lines might approach and possibly cross each other in an independent manner. Instead,  $T_{IT}$  merges with  $T_C$  at  $x = 0.06$  with a noticeable kink around  $x \sim 0.1$ . The  $T_{IT}$  line seems "attracted" by  $T_C$ , as if the tilt instability were favored by the ferroelectric one. On the other hand, also  $T_C$  may feel some effect from the proximity with  $T_{IT}$ , since its slope slightly decreases after joining with  $T_{IT}$  below  $x \sim 0.05$ . It appears that both  $T_{IT}$  and  $T_C$  increase with respect to the trend extrapolated from higher  $x$ , when they are far from each other. This is shown in Fig. 8, where the dashed lines are the extrapolations (with no pretension of quantitative analysis) of  $T_C$  and  $T_T$ . The vertical arrows are the maximum deviations of the actual  $T_C$  and  $T_{IT}$  lines from their extrapolations,  $\Delta T_C \sim 16$  K and  $\Delta T_T \sim 48$  K. A possible qualitative explanation of this observations is in terms of cooperation between a stronger FE instability and a weaker AFD tilt instability. The FE mode leaves the lattice unstable also below  $T_C$ , since its restiffening is gradual, and also affects the modes coupled to it, in particular favoring the condensation of modes cooperatively coupled to it at a temperature higher than in the normal stiff lattice away from  $T_C$ . The rotations of the octahedra are certainly coupled with the polar modes, as demonstrated by the polarization<sup>51,52</sup> and dielectric<sup>7,53</sup> anomalies at the tilt transitions, and the issue whether this coupling is cooperative or competitive is discussed in Sect. IV G. Assuming that the first eventuality is true, one has a mechanism that enhances  $T_{IT}$  in the proximity

of  $T_C$ , but the coupling works also in the other sense: the proximity of the tilt instability favors the condensation of the FE mode, enhancing  $T_C$ . The energies involved in the FE instability are larger than those involved in tilting, as indicated by the fact that  $T_C > T_T$ , and accordingly the perturbation of the FE mode on the tilt mode is larger:  $\Delta T_T \sim 3\Delta T_C$ .

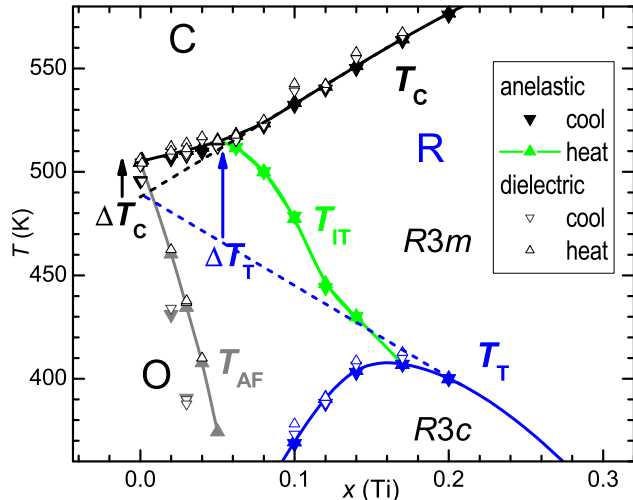


FIG. 8: Zr-rich region of the phase diagram based on our anelastic and dielectric spectra. The dashed lines are extrapolations from the high- $x$  behavior of  $T_C(x)$  and  $T_T(x)$ . The arrows  $\Delta T_C$  and  $\Delta T_T$  represent the deviation from the extrapolated behavior.

#### D. Kinks in the $T_{MPB}$ and $T_T$ lines

Other new features of the PZT phase diagram that derive from the present data are the approaches of the  $T_{MPB}(x)$  line with  $T_T$  and  $T_C$ , and a distinct kink in  $T_T$  when encounters  $T_{MPB}$ . This is better seen in the detail of the MPB region in Fig. 9, where, besides the same data of Fig. 6, other points of  $T_{MPB}$  and  $T_T$  are reported from the literature. The data are from diffraction<sup>8</sup> ( $\diamond$ ) piezoelectric coefficient<sup>54</sup>  $d_{11}$  ( $\square$ ),  $1/s_{11}$  measured with piezoelectric resonance<sup>55</sup> ( $\circ$ ), Raman<sup>9</sup> ( $-$ ), dielectric ( $+$ ) and infrared ( $\times$ )<sup>21</sup> spectroscopies.

Let us first consider how  $T_T(x)$  enters the MPB region. The points from the literature, obtained from different techniques and samples, are rather sparse, but those from our anelastic and dielectric spectra have little dispersion, and show a clear change of slope of  $T_T(x)$  when it approaches  $T_{MPB}$  at  $0.487 < x < 0.494$ . This narrow composition range is close to but not the same over which the anomaly in  $Q^{-1}$  changes between cusped and step-like (Fig. 5). In fact that change, marked by arrows in Fig. 9, occurs at  $x \lesssim 0.48$ , and therefore the two changes may depend on different mechanisms. We will discuss the transition in the shape of the  $Q^{-1}$  anomaly in Sect. IV H, and now we focus on the kink in the  $T_T$  line, which

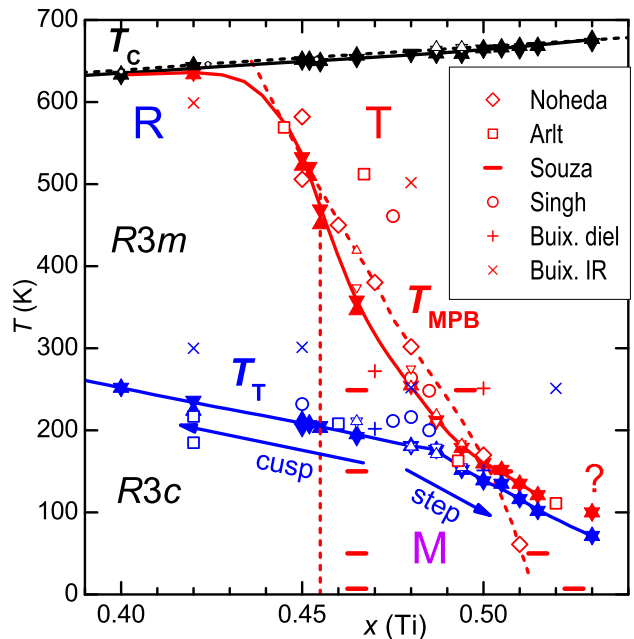


FIG. 9: Enlargement of the MPB region of the phase diagram of PZT. Triangles and solid lines from our measurements, as in Fig. 6. Dashed lines and diamonds from Noheda and other open symbols as indicated in the legend. The shape of the continuous  $T_{MPB}(x)$  line between  $x = 0.42$  and  $0.45$  is hypothetical.

we think is closely connected with the proximity to the MPB.

Also our  $T_{MPB}$  points draw a curve with little dispersion, compared to the body of data in the literature, but in this case a difference emerges in the low temperature region: even though with only three points below 100 K, the data from diffraction<sup>8</sup> and Raman<sup>9</sup> define an almost straight MPB border that ends at  $T = 0$  at  $x = 0.520 \pm 0.005$ . Instead, our data define a curved line that never crosses  $T_T$ . Our closely spaced points in the phase diagram and the regular evolution of the spectra from which they are obtained (Figs. 4 and 5) suggest that the effect is real and characteristic of good quality ceramic samples. The last point with the question mark, obtained from the dashed curve in Fig. 4, probably does not correspond to  $T_{MPB}$ , but the difference remains at  $x = 0.515$  between our curve at 120 K, and two points at 50 – 60 K from diffraction and Raman scattering. These discrepancies may depend on differences in the samples rather than on the experimental technique. In fact, the existence of the intermediate monoclinic phase and its nature are not yet unanimously accepted, and it is also proposed that, besides nanoscale twinning, defect structures like planes of O vacancies may have a role in defining the microstructure of PZT and act as nuclei for intermediate phases.<sup>56</sup> Hence, there is a range of microstructures that may well reflect in the position of the MPB, but, again, the consistency and regularity of the data encourage to consider the features presented here as intrinsic of the

PZT phase diagram and not vagaries from uncontrolled defects.

It results that also  $T_T$  and  $T_{MPB}$  almost coincide over an extended composition range, with  $T_{MPB}$  seemingly pushed up by  $T_T$ . For  $x > 0.49$ ,  $T_{MPB}$  deduced from the maximum in  $s'$  and  $T_T$  deduced from the step in  $Q^{-1}$  run parallel and close to each other and it is difficult to assess whether they still represent two distinct transitions or instead they are the manifestations of a same combined polar and tilt transition.

### E. Merging of tilt and polar instabilities also in NBT-BT

Another example in which tilt instability lines merge with polar instability lines is  $(\text{Na}_{1/2}\text{Bi}_{1/2})_{1-x}\text{Ba}_x\text{TiO}_3$  (NBT-BT).<sup>57</sup> This system has much stronger chemical disorder than PZT and a more complicated and less defined phase diagram, especially beyond the MPB composition  $x(\text{Ba}) > 0.06$ , where the correlation lengths are so short to render the material almost a relaxor. In Fig. 10 the phase diagram of NBT-BT is presented together with that of PZT. The broken lines represent the borders between regions with different tilts, while the solid lines are polar instabilities ( $T_{AF}$  in PZT is both tilt and polar). The regions where two types of instabilities merge are vertically hatched, while differently slanted hatches represent different tilt patterns. In NBT the tolerance factor is small due to the smallness of the mean A ion size of  $\text{Na}^+$  and  $\text{Bi}^{3+}$  combined, and is increased by substituting with Ba. Tilting occurs in two stages, first  $a^0a^0c^+$  (T phase) below  $T_1$  and then  $a^-a^-a^-$  (R) below  $T_2$ , and both  $T_1$  and  $T_2 + T_{MPB}$  have negative  $dT/dx$ , so enclosing the low temperature/low tolerance factor region of the phase diagram, as discussed in Sect. IV A (the  $T_1$  line actually disappears into a highly disordered relaxor-like region). At variance with PZT, the polar instabilities occur at temperatures lower than those of tilting, and in two stages: first an almost AFE or ferrielectric region below a temperature  $T_m$  signaled by a maximum in the dielectric susceptibility, and then FE below the so-called depolarization temperature  $T_d$ . The intermediate  $\sim$ AFE structure is due to shifts of the Ti and Bi cation along [001] in opposite directions, so to make  $P$  almost null, and therefore is not the result of coupling with the AFD  $a^0a^0b^+$  tilting.<sup>58</sup> The FE phase, however, appears below a  $T_d < T_2$  at  $x = 0$ , which rises and merges with the decreasing  $T_2(x)$  at  $x = 0.02$ <sup>57</sup> or  $0.03$ .<sup>59</sup> Beyond 6% Ba, the  $T_d$  and  $T_2 \equiv T_{MPB}$ , the latter ill defined, separate again. As a result, the border  $T_d$  to the FE phase, instead of simply crossing  $T_2$ , merges with it in the range  $0.02 < x < 0.06$ , following a wavy path.

Similarly to the cases of  $T_{IT}/T_C$  and  $T_C/T_{MPB}$  in PZT, the coincidence of  $T_d$  and  $T_2$  in the composition range  $0.02 < x(\text{Ba}) < 0.06$  may be interpreted as a manifestation of cooperative coupling between tilt and FE instabilities. Interestingly, like  $\text{Pb}^{2+}$  also  $\text{Bi}^{3+}$  has a lone pair

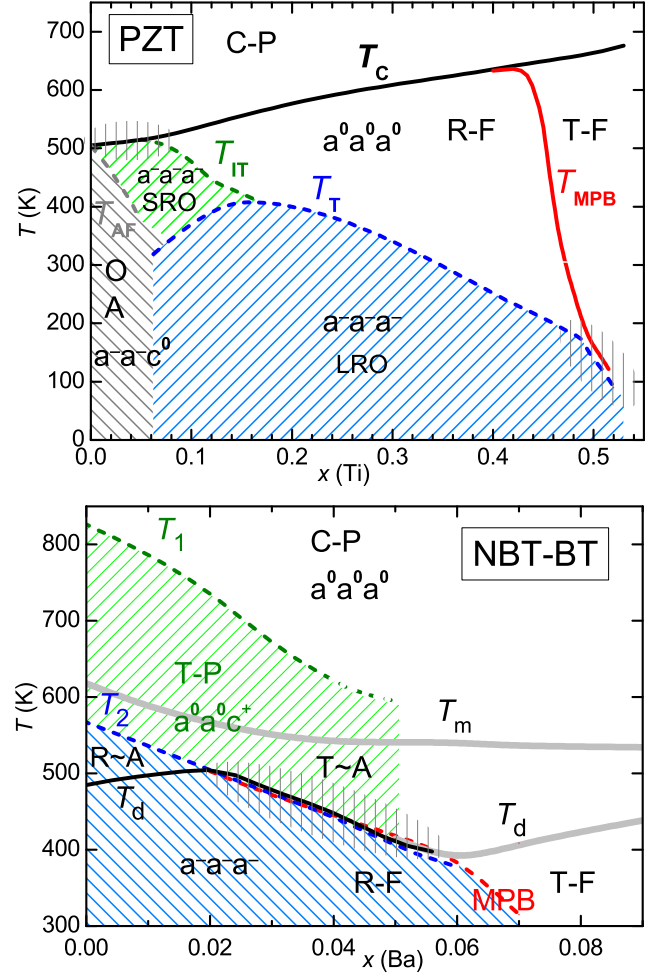


FIG. 10: Phase diagrams of PZT and NBT-BT,<sup>57</sup> where the broken lines are tilt instability borders, while the solid lines are polar instability borders. Vertical hatching evidences the regions where the two types of lines merge. Differently slanted patterns represent different tilt patterns. P, F and A stand for paraelectric, ferroelectric and antiferroelectric; SRO and LRO stand for short/long range order.

electronic configuration, with the tendency to reduce its coordination number and form short bonds with covalent character<sup>58,60</sup> which couple tilt and polar modes.<sup>61</sup>

### F. Merging of tilt and polar instabilities: trigger type transitions?

A possible mechanism for the merging of two transitions with different order parameters, whose lower order coupling term is biquadratic, had been proposed by Holakowský.<sup>62</sup> This is also the case of octahedral tilting, whose order parameter is the rotation angle  $\omega$ , and polar or antipolar modes with order parameter  $P$  (all one-dimensional for simplicity). In the Landau expansion of the free energy, terms of the type  $\omega P$ ,  $\omega P^2$  and  $\omega^2 P$

are not invariant under all symmetry operations in the symmetric phase, and therefore are forbidden; the lowest order term that contains both  $P$  and  $\omega$  is  $\gamma P^2 \omega^2$ .<sup>63</sup> In a FE transition triggered by the order parameter  $\omega$ ,<sup>62</sup> the equilibrium value of  $\omega$  is expressed in terms of  $P$  and the Landau free energy is written only in terms of  $P$ , so that the coupling term renormalizes the term quartic in  $P$  (and viceversa the term quartic in  $\omega$  is renormalized if one considers that  $P$  triggers  $\omega$ ). If the coupling coefficient  $\gamma$  is sufficiently large and negative, it can make the term  $\propto P^4$  negative and induce a combined transition of both order parameters  $P$  and  $\omega$  at a temperature higher than those at which either of them would become unstable separately. The case of the  $T_C$  and  $T_T + T_{TT}$  lines of PZT is more complicated, since the triggered transition does not produce a phase with a clear symmetry of the polar and tilt order parameters, apparently because the energy shifts from chemical disorder compete with the energies involved in the regular Landau expansion of a homogeneous crystal. Yet, the triggered phase transition mechanism<sup>62</sup> may well be at the origin of the anomalous rise and merging in temperature of the tilt and FE instabilities. In addition, a coupling term  $\gamma P^2 \omega^2$  with  $\gamma$  large and negative would renormalize the term  $\frac{1}{2} \varepsilon^{-1} P^2$ , reducing it when the average value of  $\omega$  increases and accounting for the positive step in the dielectric susceptibility below  $T_T$ .

Although a more detailed analysis would be necessary, we suggest that the same mechanism might be responsible for the coincidence of the  $T_{MPB}$  and  $T_T$  lines, now considering as FE order parameter the transversal component of  $P$ , responsible for the rotation of the polarization away from the tetragonal axis. The mechanism of the trigger-type transition has been applied so far to very few cases, like  $\text{Bi}_4\text{Ti}_3\text{O}_{12}$ <sup>64</sup> and recently proposed to explain the sequence of phase transitions of the multiferroic  $\text{BiFeO}_3$ ,<sup>65</sup> and is therefore considered as very rare.<sup>65</sup> The possibility that a trigger-type mechanism is also responsible for the particular features of the phase diagrams of PZT and NBT-BT suggests that it may be not so rare.

Finally,  $T_{MPB}$  seems to join also  $T_C$  smoothly, although the upper end of the  $T_{MPB}$  line in the phase diagrams above is based on only one datum and largely hypothetical (but similar to that of Ref. 32). This case is different from the previous ones, since the order parameter active below  $T_{MPB}$  is not independent from that active at  $T_C$ , both being the polarization, and a triggered phase transition would be meaningless. Anyway, the manner in which  $T_{MPB}$  meets  $T_C$  deserves further investigation.

### G. Competition or cooperation of tilt and polar modes?

The interpretation above contrasts with the widespread opinions that the coupling between tilt and polar modes is negligible or competitive, and therefore it is opportune to discuss the nature of the

interaction between polar and tilt modes.

#### 1. Negligible tilt-polarization coupling

In the context of the general trends of the perovskite phase diagrams at different compositions, the coupling between tilting and deformation or polar modes has been considered negligible in rhombohedral perovskites.<sup>66</sup> This assumption was based on the observation that in a large number of rhombohedral perovskites, including FE ones, the rotation angle  $\omega$  of the octahedra and the polyhedral volume ratio mentioned in Sect. IV A are related by

$$V_A/V_B = 6 \cos^2 \omega - 1, \quad (1)$$

which is valid in the absence of octahedral distortions. In other words, the tilt angles are independent of the distortions,<sup>66</sup> which necessarily occur in the FE phases. This fact, however, shows that the mismatch between the bond lengths or polyhedral volumes is accommodated almost exclusively by the tilting mechanism, and this is understandable, since the only two normal modes producing a large change of  $V_A/V_B$  are in-phase and anti-phase rotations of the octahedra, while all the other modes yield distortions with little change of  $V_A/V_B$ .<sup>35</sup> Therefore, while the validity of Eq. (1) is a manifestation of the fact that  $V_A/V_B$  depends almost exclusively on the tilting angle  $\omega$ , it does not imply a lack of coupling between tilting and the other distortion and displacement modes, for example influencing the type of tilt correlations.

#### 2. Competitive tilt-polarization coupling

The most widely accepted view is of a competition between FE and AFD instabilities, based on their opposite behavior under pressure.<sup>67-70</sup> Indeed, in titanates and other perovskites pressure suppresses FE and promotes tilting, and this can be simplistically understood in terms of a steric mechanism: FE requires more space for cation off-centering while the octahedral rotation is promoted by a compression of the lattice that amplifies the mismatch between B-O and A-O sublattices. These observations, however, show that the two instabilities behave in opposite manner under pressure, but not necessarily that they compete against each other. It should also be noted that there are several exceptions to the "rule" that pressure favors tilting, for example perovskites with trivalent B = Al,<sup>71</sup> Gd,<sup>72</sup> and there are even studies that assume that the general rule is just the opposite: pressure induces the more symmetric cubic structure.<sup>73</sup> These different behaviors under pressure depend on the relative compressibilities of the  $\text{AO}_{12}$  and  $\text{BO}_6$  polyhedra, which can be rationalized in terms of the bond valence sum concept.<sup>74</sup> It appears that in the zirconates and titanates the  $\text{BO}_6$  octahedra are stiffer than the  $\text{AO}_{12}$  cuboctahedra, which is the usual case when B has larger valence than A.

Another strong and widely accepted<sup>70</sup> indication of competitive AFD-FE interaction comes from simulations<sup>75</sup> on SrTiO<sub>3</sub> showing that the FE mode of cation displacements along  $\langle 111 \rangle$  and the AFD anti-phase tilt modes compete against each other. The simulations are done on SrTiO<sub>3</sub>, which actually is not ferroelectric due to quantum fluctuations, but their result is clear: neglecting quantum fluctuations, the temperature of the tilt instability is 25% higher if the FE mode is frozen, while  $T_C$  is 20% higher if the AFD mode is frozen. This means that the two modes tend to cancel each other rather than cooperate, and the microscopic mechanism is identified in the mutual anharmonic interaction. The behavior of  $T_C$  and  $T_T$  in PZT or  $T_d$  and  $T_2$  in NBT-NT, however, seems the opposite. It is possible that the nature of interaction between AFD and FE modes is different when the A ion is Pb instead of Sr, since the difference is not only of ionic size but there is also a more strongly covalent character of the bond when Pb goes off center.<sup>58,60</sup> The other difference between the SrTiO<sub>3</sub> and PZT case is that in the first only the  $z$  component of the  $R_4$  mode becomes unstable, leading to a T structure, while in PZT all three components yield the R structure. It is therefore unlikely that the simulation of SrTiO<sub>3</sub> can be plainly generalized to Pb compounds. Rather, it may be more appropriate to refer to similar simulations<sup>65</sup> on multiferroic BiFeO<sub>3</sub>, where also Bi<sup>3+</sup> has the stereoactive lone pair like Pb<sup>2+</sup>. Such simulations indicate that the sequence of FE and AFD transitions is indeed dominated by the trigger-type mechanism, and that the coupling between the two types of modes is strong and both competitive and cooperative, due to the fact that the order parameters are multicomponent.<sup>65</sup>

### 3. Cooperative tilt-polarization coupling

That the tilts are coupled with polar modes is demonstrated by the fact that below  $T_T$  there is a positive step in the real part of the dielectric susceptibility,<sup>7,18,46</sup> as also shown in Fig. 1, and in the polarization.<sup>51</sup> The fact that both  $\chi'$  and  $P$  increase below  $T_T$  demonstrates that the interaction is cooperative. If the modes competed against each other, then the onset of tilting should depress rather than enhance the polarization and its derivative, and this is well exemplified by a biquadratic coupling term  $-|\gamma|\omega^2 P^2$ , as discussed in Sect. IV E. A detailed microscopic mechanism for cooperative interaction between polar and AFD modes has not been proposed, to our knowledge, but another indication of its existence is the fact that the application of an electric field in PZT modified with Sn and Nb enhances  $T_T$  of few degrees.<sup>76</sup> In addition, as mentioned above, strong and cooperative coupling results from first-principle based simulation of BiFeO<sub>3</sub>.<sup>65</sup>

Finally, we mention that, since direct coupling between polar and AFD modes (linear in at least either

of the two) in the ideal cubic perovskite is forbidden by symmetry, some indirect mechanisms through rotostric-tive coupling or gradient interactions (originating from the chemical disorder) had already been proposed to explain the influence of the tilt transition on the dielectric susceptibility.<sup>46</sup> The coupling between FE and AFD modes has also been discussed in relation with the appearance of new Raman<sup>77,78</sup> and infra-red<sup>21</sup> modes below  $T_T$ .

We think that the fact that tilt and polar instability lines merge over extended composition ranges instead of crossing each other are due to a cooperative coupling between polar/antipolar and tilt modes. It is interesting to note that a simulation of the PZT phase diagram including tilt degrees of freedom has already been done,<sup>17</sup> and the  $T_{MPB}$  line, though finally crosses  $T_T$ , presents a marked bend on approaching it, exactly as deduced from our anelastic and dielectric experiments.

### H. Transition in the shape of the $Q^{-1}$ anomaly at $T_T$ : the R/M border?

As already noted in Sect. IV D, the kink in the  $T_T$  line and the transition in the shape of the  $Q^{-1}$  anomaly (Fig. 5) appear at slightly different compositions, suggesting that the latter may have a different origin from the proximity to the MPB and hence polarization-tilt coupling.

If this were the case, the most obvious explanation for the change of the  $Q^{-1}$  anomaly would be the postulated border separating R and M phases.<sup>8,9,17</sup> The existence of this border is one of the yet unsettled issues on the phase diagram of PZT, since there are various diffraction studies, also recent and on single crystals,<sup>23,30</sup> whose Rietveld refinements strongly suggest that the R and M phases coexist at least down to  $x = 0.4$ , so excluding a definite phase border. In addition, according to the view that the M phase is actually a nanotwinned R or T phase,<sup>5,6</sup> this border would not exist. Therefore, a R/M border would be highly significant: it would imply the existence of a long range M phase. A puzzling feature of this border would be its verticality. In fact, a truly vertical phase boundary in the  $x - T$  phase diagram would be understandable at a specific composition that allows a phase to be formed with commensurate cation order. This is certainly not the case of the postulated R/M border in PZT, where no Zr/Ti ordering has ever been observed, and anyway  $x \simeq 0.47$  is too far from the closest relevant composition  $x = \frac{1}{2}$ . Indeed, the R/M boundary found by first principles based simulations is not vertical: it starts at a triple point with  $T_C$  and  $T_{MPB}$  at  $x_1 = 0.463$  and ends at  $T = 0$  and  $x_2 = 0.476$ .<sup>17</sup> No experimental evidence exists so far of the crossing of such a border with change of temperature, and the change of the shape of the  $Q^{-1}$  anomaly between 0.465 and 0.48 is not a conclusive evidence of its existence, since it might be associated with a change of the character of the transition through polarization-tilt coupling near the MPB. Further experi-

ments at more closely spaced compositions are necessary to ascertain this point.

## V. CONCLUSIONS

Anelastic and dielectric measurements are reported at compositions of the phase diagram of  $\text{PbZr}_{1-x}\text{Ti}_x\text{O}_3$  near the two morphotropic phase boundaries (MPB) of the rhombohedral phase with the tetragonal and the orthorhombic phases. Several new features are found in both regions, and discussed in terms of octahedral tilting and cooperative coupling between the tilt and polar/antipolar modes.

We confirm the recent discovery<sup>7</sup> of a new phase transition at a temperature  $T_{\text{IT}}$  that prosecutes the border  $T_{\text{T}}$  of the tilt instability up to the Curie temperature  $T_{\text{C}}$ , in the region where  $T_{\text{T}}$  drops and meets the border with the orthorhombic antiferroelectric phase. The new phase is assumed to represent the initial stage of octahedral tilting, without long range order due to the enhanced cation disorder near the AFE border. Lacking evidence from diffraction for this intermediate tilt region, the rationale for the assumption that tilting is involved is discussed in terms of mismatch between the networks of Pb-O and (Zr/Ti)-O bonds, as usual for tilted perovskites. In addition, it is proposed that, due to the anisotropy of the correlation length of different types of tilts, the initial stage of tilting in the presence of disorder involves flat clusters of octahedra rotating about  $\langle 100 \rangle$  axes, so producing  $\frac{1}{2} \langle 110 \rangle$  type modulations, even

when the final long range modulation is of  $\frac{1}{2} \langle 111 \rangle$  type.

The  $T_{\text{IT}}$  tilt instability line merges with the ferroelectric  $T_{\text{C}}$  with an evident step and both temperatures appear enhanced with respect to the extrapolations from the region where they are far from each other. Also the  $T_{\text{T}}$  line presents a clear kink when it meets the MPB and, contrary to previous experiments,  $T_{\text{MPB}}$  is found to deviate and go parallel or even merge with  $T_{\text{T}}$ , instead of crossing it. These observations of deviations and merging of tilt and polar instability borders are compared to a similar example in NBT-BT, and explained in terms of strong and cooperative interaction between the polar and the tilt modes, which causes a trigger type transition. Since the prevalent opinions are that tilt-polarization coupling is competitive or negligible, and the trigger-type transitions are extremely rare, the various indications of polar-tilt coupling in PZT are reviewed and discussed.

Another feature that is considered is a rather abrupt transition in the shape of the anomaly in the elastic losses at  $T_{\text{T}}$ . The anomaly is a peak or cusp for  $x \leq 0.465$  and a step for  $x \geq 0.48$ . The possibility is discussed that between these two compositions there is an actual border between rhombohedral and monoclinic phases.

### Acknowledgments

The authors thank Mr. C. Capiani (ISTEC) for the skillful preparation of the samples, Mr. P.M. Latino (ISC) and A. Morbidini (INAF) for their technical assistance in the anelastic and dielectric experiments.

- 
- <sup>1</sup> E. Sawaguchi, J. Phys. Soc. Jpn. **8**, 615 (1953).  
<sup>2</sup> H. Jaffe, Proc. IEE, B Electron. Commun. Eng. UK **109**, 351 (1962).  
<sup>3</sup> B. Jaffe, W.R. Cook and H. Jaffe, *Piezoelectric Ceramics*. (Academic Press, London, 1971).  
<sup>4</sup> B. Noheda, D.E. Cox, G. Shirane, L.E. Cross and S.-E. Park, Appl. Phys. Lett. **74**, 2059 (1999).  
<sup>5</sup> A.G. Khachatryan, Phil. Mag. **90**, 37-60 (2010).  
<sup>6</sup> K.A. Schönau, L.A. Schmitt, M. Knapp, H. Fuess, R.-A. Eichel, H. Kungl and M.J. Hoffmann, Phys. Rev. B **75**, 184117 (2007).  
<sup>7</sup> F. Cordero, F. Trequattrini, F. Craciun and C. Galassi, J. Phys.: Condens. Matter **23**, 415901 (2011).  
<sup>8</sup> B. Noheda, D.E. Cox, G. Shirane, R. Guo, B. Jones and L.E. Cross, Phys. Rev. B **63**, 014103 (2000).  
<sup>9</sup> A.G. Souza Filho, K.C.V. Lima, A.P. Ayala, I. Guedes, P.T.C. Freire, F.E.A. Melo, J. Mendes Filho, E.B. Araújo and J.A. Eiras, Phys. Rev. B **66**, 132107 (2002).  
<sup>10</sup> H.D. Megaw, Proc. Royal Soc. **58**, 133 (1946).  
<sup>11</sup> P.M. Woodward, Acta Cryst. B **53**, 44 (1997).  
<sup>12</sup> I.M. Reaney, E.L. Colla and N. Setter, Jpn. J. Appl. Phys. **33**, 3984-3990 (1994).  
<sup>13</sup> D.I. Woodward, J. Knudsen and I.M. Reaney, Phys. Rev. B **72**, 104110 (2005).  
<sup>14</sup> I.D. Brown, Acta Cryst. B **48**, 553 (1992).  
<sup>15</sup> I.D. Brown, A. Dabkowski and A.A. McCleary, Acta Cryst. B **53**, 750 (1997).  
<sup>16</sup> A.M. Glazer, Acta Cryst. B **28**, 3384 (1972).  
<sup>17</sup> I.A. Kornev, L. Bellaiche, P.-E. Janolin, B. Dkhil and E. Suard, Phys. Rev. Lett. **97**, 157601 (2006).  
<sup>18</sup> F. Cordero, F. Craciun and C. Galassi, Phys. Rev. Lett. **98**, 255701 (2007).  
<sup>19</sup> M. Hinterstein, K.A. Schoenau, J. Kling, H. Fuess, M. Knapp, H. Kungl and M.J. Hoffmann, J. Appl. Phys. **108**, 024110 (2010).  
<sup>20</sup> M. Deluca, H. Fukumura, N. Tonari, C. Capiani, N. Haisuie, K. Kisoda, C. Galassi and H. Harima, J. Raman Spectr. **42**, 488 (2011).  
<sup>21</sup> E. Buixaderas, D. Nuzhnyy, J. Petzelt, L. Jin and D. Damjanovic, Phys. Rev. B **84**, 184302 (2011).  
<sup>22</sup> R. Ranjan, A.K. Singh, Ragini and D. Pandey, Phys. Rev. B **71**, 092101 (2005).  
<sup>23</sup> D. Phelan, X. Long, Y. Xie, Z.-G. Ye, A.M. Glazer, H. Yokota, P.A. Thomas and P.M. Gehring, Phys. Rev. Lett. **105**, 207601 (2010).  
<sup>24</sup> R. Singh Solanki, A. Kumar Singh, S.K. Mishra, S.J. Kennedy, T. Suzuki, Y. Kuroiwa, C. Moriyoshi and D. Pandey, Phys. Rev. B **84**, 144116 (2011).  
<sup>25</sup> F. Cordero, L. Dalla Bella, F. Corvasce, P.M. Latino and A. Morbidini, Meas. Sci. Technol. **20**, 015702 (2009).

- <sup>26</sup> A.S. Nowick and B.S. Berry, *Anelastic Relaxation in Crystalline Solids*. (Academic Press, New York, 1972).
- <sup>27</sup> W. Rehwald, *Adv. Phys.* **22**, 721 (1973).
- <sup>28</sup> M.A. Carpenter and E.H.K. Salje, *Eur. J. Mineral.* **10**, 693-812 (1998).
- <sup>29</sup> R. G. Burkovsky, Yu. A. Bronwald, A. V. Filimonov, A. I. Rudskoy, D. Chernyshov, A. Bosak, J. Hlinka, X. Long, Z.-G. Ye, S. B. Vakhrushev, arXiv:1204.5878v1 (2012).
- <sup>30</sup> H. Yokota, N. Zhang, A.E. Taylor, P.A. Thomas and A.M. Glazer, *Phys. Rev. B* **80**, 104109 (2009).
- <sup>31</sup> N. Zhang, H. Yokota, A.M. Glazer and P.A. Thomas, *Acta Cryst. B* **67**, 386 (2011).
- <sup>32</sup> E.G. Fesenko, V.V. Eremkin and V.G. Smotrakov, *Sov. Phys. Solid State* **28**, 181 (1986).
- <sup>33</sup> R.D. Shannon, *Acta Cryst. A* **32**, 751-767 (1976).
- <sup>34</sup> N.W. Thomas, *Acta Cryst. B* **45**, 337 (1989).
- <sup>35</sup> D. Wang and R.J. Angel, *Acta Cryst. B* **67**, 302 (2011).
- <sup>36</sup> C.J. Howard and H.T. Stokes, *Acta Cryst. B* **54**, 782 (1998).
- <sup>37</sup> R.E. Eitel, C.A. Randall, T.R. Shrout, P.W. Rehrig, W. Hackenberger and S.-E. Park, *Jpn. J. Appl. Phys.* **40**, 5999-6002 (2001).
- <sup>38</sup> M.R. Suchomel and P.K. Davies, *J. Appl. Phys.* **96**, 4405 (2004).
- <sup>39</sup> W.-C. Lee, C.-Y. Huang, L.-K. Tsao and Y.-C. Wu, *J. Eur. Ceram. Soc.* **29**, 1443 (2009).
- <sup>40</sup> H. Zheng, I.M. Reaney, W.E. Lee, N. Jones and H. Thomas, *J. Am. Ceram. Soc.* **85**, 2337 (2002).
- <sup>41</sup> J. Burgy, M. Mayr, V. Martin-Mayor, A. Moreo and E. Dagotto, *Phys. Rev. Lett.* **87**, 277202 (2001).
- <sup>42</sup> E. Dagotto, *New J. Phys.* **7**, 67 (2005).
- <sup>43</sup> D.L. Corker, A.M. Glazer, R.W. Whatmore, A. Stallard and F. Fauth, *J. Phys.: Condens. Matter* **10**, 6251 (1998).
- <sup>44</sup> J. Hlinka, P. Ondrejko, M. Kempa, E. Borissenko, M. Krisch, X. Long and Z.-G. Ye, *Phys. Rev. B* **83**, 140101 (2011).
- <sup>45</sup> D. Viehland, *Phys. Rev. B* **52**, 778 (1995).
- <sup>46</sup> D. Viehland, J.-F. Li, X. Da and Z. Xu, *J. Phys. Chem. Sol.* **57**, 1545 (1996).
- <sup>47</sup> J. Ricote, D.L. Corker, R.W. Whatmore, S.A. Impey, A.M. Glazer, J. Dec and K. Roleder, *J. Phys.: Condens. Matter* **10**, 1767 (1998).
- <sup>48</sup> Y. Kuroiwa, Y. Terado, S.J. Kim, A. Sawada, Y. Yamamura, S. Aoyagi, E. Nishibori, M. Sakata and M. Takata, *Jpn. J. Appl. Phys.* **44**, 7151 (2005).
- <sup>49</sup> B. Ravel and E.A. Stern, *Physica B* **208&209**, 316 (1995).
- <sup>50</sup> P. Sollich, V. Heine and M.T. Dove, *J. Phys.: Condens. Matter* **6**, 3171 (1994).
- <sup>51</sup> R.W. Whatmore, R. Clarke and A.M. Glazer, *J. Phys. C: Solid State Phys.* **11**, 3089-3102 (1978).
- <sup>52</sup> N. Cerereda, B. Noheda, T. Iglesias, J.R. Fernandez - del Castillo, J.A. Gonzalo, N. Duan, Y.L. Wang, D.E. Cox and G. Shirane, *Phys. Rev. B* **55**, 6174 (1997).
- <sup>53</sup> X. Dai, Z. Xu, J.-F. Li and D. Viehland, *J. Appl. Phys.* **77**, 3354 (1995).
- <sup>54</sup> G. Arlt, *Proc. IEEE Ultrasonic Symposium*, 733 (1990).
- <sup>55</sup> A.K. Singh, S.K. Mishra, agini, D. Pandey, S. Yoon, S. Baik and N. Shin, *Appl. Phys. Lett.* **92**, 022910 (2008).
- <sup>56</sup> L.A. Reznichenko, L.A. Shilkina, O.N. Razumovskaya, E.A. Yaroslavtseva, S.I. Dudkina, O.A. Demchenko, Yu.I. Yurasov, A.A. Esis and I.N. Andryushina, *Phys. Solid State* **51**, 1010 (2009).
- <sup>57</sup> F. Cordero, F. Craciun, F. Trequattrini, E. Mercadelli and C. Galassi, *Phys. Rev. B* **81**, 144124 (2010).
- <sup>58</sup> G.O. Jones and P.A. Thomas, *Acta Cryst. B* **58**, 168-178 (2002).
- <sup>59</sup> Y. Hiruma, Y. Watanabe, H. Nagata and T. Takenaka, *Key Eng. Mater.* **350**, 93-96 (2007).
- <sup>60</sup> I.-W. Chen, P. Li and Y. Wang, *J. Phys. Chem. Sol.* **57**, 1525 (1996).
- <sup>61</sup> Ph. Ghosez, E. Cockayne, U.V. Waghmare and K.M. Rabe, *Phys. Rev. B* **60**, 836 (1999).
- <sup>62</sup> J. Holakovský, *phys. stat. sol. (b)* **56**, 615 (1973).
- <sup>63</sup> M.J. Haun, E. Furman, S.J. Jang and L.E. Cross, *Ferroelectrics* **99**, 13-25 (1989).
- <sup>64</sup> J. Holakovský, *phys. stat. sol. (b)* **69**, 615 (1975).
- <sup>65</sup> I.A. Kornev and L. Bellaiche, *Phys. Rev. B* **79**, 100105 (2009).
- <sup>66</sup> N.W. Thomas and A. Beitollahi, *Acta Cryst. B* **50**, 549 (1994).
- <sup>67</sup> G.A. Samara, T. Sakudo and K. Yoshimitsu, *Phys. Rev. Lett.* **35**, 1767 (1975).
- <sup>68</sup> J. Kreisel, B. Noheda and B. Dkhil, *Phase Trans.* **82**, 633 (2009).
- <sup>69</sup> J. Frantti, Y. Fujioka, J. Zhang, S.C. Vogel, Y. Wang, Y. Zhao and R.M. Nieminen, *J. Phys. Chem. B* **113**, 7967 (2009).
- <sup>70</sup> G. Frayssse, A. Al-Zein, J. Haines, J. Rouquette, V. Bornand, P. Papet, C. Bogicevic and S. Hull, *Phys. Rev. B* **84**, 144110 (2011).
- <sup>71</sup> N. L. Ross, Zhao and R. J. Angel, *J. Solid State Chem.* **177**, 1276 (2004).
- <sup>72</sup> J. Zhao, N.L. Ross and R.J. Angel, *Acta Cryst. B* **60**, 263 (2004).
- <sup>73</sup> B. Magyari-Köpe, L. Vitos, B. Johansson and J. Kollár, *Phys. Rev. B* **66**, 092103 (2002).
- <sup>74</sup> R.J. Angel, J. Zhao and N.L. Ross, *Phys. Rev. Lett.* **95**, 025503 (2005).
- <sup>75</sup> W. Zhong and D. Vanderbilt, *Phys. Rev. Lett.* **74**, 2587 (1995).
- <sup>76</sup> P. Yang, M.A. Rodriguez, G.R. Burns, M.E. Stavig and R.H. Moore, *J. Appl. Phys.* **95**, 3626-3632 (2004).
- <sup>77</sup> D. Wang, J. Weerasinghe, L. Bellaiche and J. Hlinka, *Phys. Rev. B* **83**, 020301 (2011).
- <sup>78</sup> J. Weerasinghe, D. Wang and L. Bellaiche, *Phys. Rev. B* **85**, 014301 (2012).